Lipoprotein-Associated Phospholipase A 2 Interacts with Phospholipid Vesicles via a Surface-Disposed Hydrophobic α-Helix

5 AUTHORS, INCLUDING:

Yuan-Hao Howard Hsu
Tunghai University
21 PUBLICATIONS 440 CITATIONS

SEE PROFILE

Sheng Li
University of California, San Diego
87 PUBLICATIONS 1,505 CITATIONS

SEE PROFILE

Lipoprotein-Associated Phospholipase A$_2$ Interacts with Phospholipid Vesicles Via a Surface-Disposed Hydrophobic α-Helix

Jian Cao[1], **Yuan-Hao Hsu**[1], **Sheng Li**[2], **Virgil L. Woods Jr.**[2], and **Edward A. Dennis**[1,*]

[1] Department of Chemistry and Biochemistry and Pharmacology, School of Medicine, University of California, San Diego, La Jolla, California 92093-0601

[2] Department of Medicine, Biomedical Sciences Graduate Program, University of California, San Diego, La Jolla, California 92093-0601

Abstract

Lipoprotein-associated phospholipase A$_2$ (Lp-PLA$_2$) plays important roles in both the inhibition and promotion of inflammation in human disease. It catalyzes the hydrolytic inactivation of plasma platelet activating factor (PAF) and is also known as PAF acetylhydrolase. High levels of PAF are implicated in a variety of inflammatory diseases such as asthma, necrotizing enterocolitis and sepsis. Lp-PLA$_2$ also associates with lipoproteins in human plasma where it hydrolyzes oxidized phospholipids to produce pro-inflammatory lipid mediators that can promote inflammation and the development of atherosclerosis. Lp-PLA$_2$ plasma levels have recently been identified as a biomarker of vascular inflammation, atherosclerotic vulnerability, and future cardiovascular events. The enzyme is thus a prominent target for the development of inflammation and atherosclerosis-modulating therapeutics. While the crystallographically-determined structure of the enzyme is known, the enzyme's mechanism of interaction with PAF and the function-modulating lipids in lipoproteins is unknown. We have employed peptide amide hydrogen-deuterium exchange mass spectrometry (DXMS) to characterize the association of Lp-PLA$_2$ with dimyristoyl phosphatidylcholine (DMPC) vesicles, and found that specific residues 113-120 in one of the enzyme's surface-disposed hydrophobic α-helices likely mediate liposome binding.

Several lines of evidence suggest important anti-inflammatory and pro-inflammatory roles for lipoprotein-associated phospholipase A$_2$ (Lp-PLA$_2$) (*1*). This enzyme associates with both low density lipoproteins (LDL) and high density lipoproteins (HDL) in human plasma *(2)*, and was first discovered based on its ability to catalyze the hydrolysis of the acetyl group at the *sn-2* position of human plasma platelet activating factor (PAF) to produce lyso-PAF and acetate. It is thus also termed PAF acetylhydrolase and belongs to the phospholipase A$_2$ (PLA$_2$) superfamily (known as GVIIA phospholipase A$_2$) (*3*). In addition to hydrolyzing PAF, Lp-PLA$_2$ also catalyzes the hydrolysis of short acyl group phospholipids, F$_2$-isoprostanes esterified phospholipids and notably oxidized phospholipids (*4-6*).

High levels of PAF are responsible for a variety of human inflammatory diseases including asthma, necrotizing enterocolitis and sepsis (*7, 8*). Because hydrolysis of the acetyl group inactivates PAF, Lp-PLA$_2$ plays an important role in the pathogenesis of acute inflammation

and deficiency of Lp-PLA$_2$ and has been found to be associated with increased risk of asthma, atherosclerosis and coronary artery disease (*9*). Four percent of the Japanese population have a Lp-PLA$_2$ loss-of-function mutant (V279F) and the deficiency of enzyme activity caused by the mutation is a risk factor for severe asthma and atopy (*10*). I198T and A379V missense mutations are also found in the European population and, while the Lp-PLA$_2$ mutants are functional, the mutations are associated with increased susceptibility to asthma and atopy *(10)*. Considerable attention has also been focused on the pro-inflammatory effects of Lp-PLA$_2$. The products of Lp-PLA$_2$ mediated hydrolysis of oxidized phospholipids, lysophosphatidylcholine and oxidized fatty acids, are bioactive pro-inflammatory lipid mediators that likely play an important roles in inflammation and in the development of atherosclerotic necrotic cores *(11)*. Lp-PLA$_2$ plasma levels have recently been identified as a biomarker of vascular inflammation, athlerosclerotic vulnerability, and predictor of cardiovascular events *(12)*. The enzyme is thus a prominent target for the development of inflammation and athlerosclerosis-modulating therapeutics.

While the crystallographically-determined structure of the enzyme is known, the enzyme's mechanism of interaction and association with the phospholipid-containing vesicles is unknown. The activity of most phospholipase A$_2$ family members critically depends on the interaction of the protein with large lipid aggregates, and thus understanding of the molecular interactions between lipid aggregates and Lp-PLA$_2$ will be important in the design of enzyme-modulating therapeutics (*13*). Lp-PLA$_2$ is a 45 kDa, Ca^{2+}-independent phospholipase A$_2$ and contains a *GXSXG* motif, which is a characteristic fingerprint of neutral lipases and serine esterases (*14*). Its crystal structure shows that Lp-PLA$_2$ contains a classic lipase/esterase α/β hydrolase fold and features a catalytic serine/ histidine/ aspartic acid triad (*15*). As PAF can partition between the aqueous phase and a lipid phase, it has been suggested that Lp-PLA$_2$ may utilize a non-interfacial activation mechanism (*16*). Alternatively, it has been assumed that under physiological conditions Lp-PLA$_2$ binds its substrate(s) while located in the lipid membrane phase as is the case for all classic membrane-associating PLA$_2$ enzymes.

The large size of lipid aggregates required for the study of lipid-enzyme interactions precludes the use of many standard biophysical analytical techniques including X-ray crystallography and solution NMR. Additionally, X-ray crystallography can only provide a static snapshot of enzyme structure, from which dynamic changes critical to functioning can at best be indirectly inferred. Peptide amide hydrogen-deuterium exchange mass spectrometry (DXMS) has been widely used to analyze protein-protein, protein-substrate, and protein-inhibitor interactions, as well as protein dynamics and protein conformational changes (*17-19*). We have previously employed DXMS to characterize the activation mechanisms of phospholipase A$_2$ superfamily members in the presence of dimyristolyphosphatidylcholine (DMPC) vesicles, including GIA secreted, GIVA cytosolic and GVIA calcium-independent PLA$_2$s (*20-24*).

Herein we have employed DXMS to characterize, at the molecular level, the association of Lp-PLA$_2$ with lipid membranes, and found that specific residues (aa 113-120) of one of the enzyme's surface-disposed hydrophobic α-helices likely mediates liposome binding.

EXPERIMENTAL PROCEDURES

Materials

D$_2$O (99.6%) was obtained from Cambridge Isotope Laboratories. [^{3}H-acteyl] PAF was purchased from Perkin Elmer. Unlabeled PAF and 1,2-dimyristoyl-*sn*-glycero-3-phosphocholine (DMPC) were from Avanti Polar Lipids (Alabaster, AL). All other reagents were analytical reagent grade or better.

Preparation of recombinant protein

The cDNA of residues 46-441 of Lp-PLA$_2$ was amplified from a full-length clone of human Lp-PLA$_2$ (Origene) by PCR and ligated into the pGS-21a vector (GenScript). The purified recombinant plasmid (GST-Lp-PLA$_2$) was confirmed by DNA sequencing (Eton Bioscience) and then was transformed into competent *E. coli* BL21(DE3) cells (Stratagene). The recombinant Lp-PLA$_2$ construct included residues 46-441 of human Lp-PLA$_2$ with an N-terminal extension of one additional alanine residue after enterokinase cleavage. This construct displays the same activity toward PAF as the natural enzyme isolated from human plasma, as the N-terminus of this protein was found heterogenerous in human blood (it can be Ser-35, Ile-42 or Lys-55) and the C-terminus is Asn-441 (*14*). Cells were grown in 1L of LB media with shaking at 37°C for 3 h, induced with 0.5 mM IPTG for an additional 4 h, and then harvested by centrifugation at 4°C. The cell pellet was suspended in PBS buffer containing 10mM CHAPS, 1mM DTT and 0.01% lysozyme. Protein extracts were obtained after 30 min incubation at room temperature in PBS buffer. The lysates were briefly sonicated and centrifuged at 20,000 g for 30 min at 4°C. The GST-Lp-PLA$_2$ fusion protein was purified by GST resin (GenScript). The GST tag was cleaved from the fusion protein via on-column cleavage using enterokinase (GenScript). After digestion, Lp-PLA$_2$ was eluted with 20 mM Tris, 150 mM NaCl, 10% glycerol, pH = 7.5, 1 mM DTT, while uncleaved GST-Lp-PLA$_2$ and cleaved GST tag still bound to the column. Enterokinase (containing 6xHis tag) was removed from the purified Lp-PLA$_2$ by Ni-NTA column chromatography (Qiagen). Purified Lp-PLA$_2$ was concentrated to 2.5mg/ml in protein buffer (20 mM Tris, 150 mM NaCl, 10% glycerol, pH 7.5, 1 mM DTT) by using Amicon Ultra-15 (Millipore) with the protein concentration determined by BCA protein assay. The cDNA of Lp-PLA$_2$ was also ligated into pET-22b and pET-45b vectors (Novagen). The 6xHis tagged proteins were expressed in *E. coli* and purified using Qiagen Ni-NTA column as the manufacturer suggested. Site-directed mutagenesis was performed as manufacturer suggested (Agilent). The mutant was purified the same as wild type protein.

Lp-PLA$_2$ activity assay

The enzyme activity was determined by a radiometric assay described elsewhere (*25*). The assay was performed in 100 mM HEPES buffer (pH = 7.5, 1 mM EGTA, 1 mM DTT, 2 mM CHAPS) by using 0.1 mM [^{3}H-acteyl] PAF as substrate in a final volume of 500 μl. The reaction was initiated by adding 1ng purified Lp-PLA$_2$ and incubated at 37°C for 20 min. The reaction was quenched using 500 μl 10 M acetic acid. The released ^{3}H-acetate was separated by C18 reversed-phase cartridges (Phenomenex) and quantitated by scintillation counting.

Preparation of DMPC small unilamellar vesicles

The DMPC lipid vesicles were prepared as described elsewhere (*26*). Briefly, DMPC (10 *m*g) was dried by N$_2$ gas and lyophilized for 1hr. The DMPC sample was then vortexed and sonicated in 1ml of PBS buffer on ice to form lipid vesicles. The solution was centrifuged at $10,000 \times$ g for 10 min to remove the large vesicles.

Lp-PLA$_2$/lipid vesicle binding experiments

The lipid binding experiments were carried out as described (*27*). Briefly 60μM DMPC vesicles containing 3 mol% N-dansyl-DHPE (Invitrogen) were mixed with various concentrations of Lp-PLA$_2$ wild-type or W115AL116A mutant protein. The resonance energy transfer from tryptophan(s) of protein to the probe N-dansyl-DHPE was monitored by TECAN M200 fluorescence photometer. Excitation was 292 nm and emission was 510 nm.

Preparation of samples for DXMS experiments

D_2O buffer consisted of 12 mM Tris, 50 mM NaCl in 99% D_2O, pD_{read} 7.5, as previously described (*20-24*). Exchange experiments were initiated by mixing 20 μL of Lp-PLA$_2$ (2.5 mg/ml) in protein buffer, or Lp-PLA$_2$ pre-incubated in 4 mM DMPC lipid vesicles, with 60 μL of D_2O buffer to a final concentration of 75% D_2O. The mixtures were incubated at 0°C for 10, 30, 100, 300, 1000, 3000 or 10,000 s and then exchange quenched by adding 120 μl of ice-cold quench solution (0.96% formic acid, 0.8 M guanidine hydrochloride (GdHCl)) resulting in samples with final concentrations of 0.58% formic acid and 0.5 M GdHCl, pH 2.5. The samples were then immediately frozen on dry ice and stored at -80°C.

Proteolysis- Liquid Chromatography-Mass Spectroscopic Analysis of Samples

All steps were performed at 0°C as described previously (*21*). In preliminary experiments, the digestion conditions of the proteins were optimized with undeuterated samples. In brief, 20 μL of Lp-PLA$_2$ in protein buffer was diluted with 60 μL of H_2O buffer, and then quenched with 120 μL of 0.96% (v/v) formic acid containing GdHCl at final concentration of 0.05, 0.5, 1.0, 2.0 and 4.0 M at 0°C. The quenched samples were snap frozen on dry ice and kept at -80°C until subjected to LC-MS analysis. The frozen samples were subsequently thawed at 4°C employing a cryogenic autosampler as previously described (*21*) and immediately passed over a immobilized pepsin column (66-μl bed volume) (*20*), at a flow rate of 100 μl/min with 0.05% trifluoroacetic acid. The eluate was directly loaded onto a C18 column (Vydac catalog number 218MS5150) and the peptides were eluted at 50 μl/min with a linear gradient of 0.046% trifluoroacetic acid, 6.4% (v/v) acetonitrile to 0.03% trifluoroacetic acid, 38.4% acetonitrile for 30 min. The eluate from the C18 column was directed to a LCQ Classic mass spectrometer (Thermo Finnigan, Inc) or ESI QTOF-I mass spectrometer (Micromass) with data acquisition in either data dependent MS2 mode or MS1 profile mode. Determination of the sequences of pepsin-generated peptides was facilitated through the use of SEQUEST (Thermo Finnigan, Inc) (*20*). The optimal peptide coverage map was obtained at a final concentration of 0.5M GdHCl in 0.58% formic acid.

Data Processing/Analysis

Data processing of hydrogen-deuterium exchange experiments utilized specialized software as previously described (DXMS Explorer, Sierra Analytics Inc.)(*20, 21*). The isotopic envelope centroids of deuterated peptides were determined from MS1 data, and converted to the deuterium incorporation into each peptide with corrections for back exchange by the equation: $D = MaxD \times (m(P)-m(N))/(m(E)-m(N))$, where $m(P)$, $m(N)$ and $m(E)$ are the centroid value of partially deuterated peptide, no-deuterated peptide, and equilibrium deuterated peptides, respectively(*28*). MaxD is the maximum LC-MS- assessable amide deuterium incorporation, calculated by subtracting the number of proline residues in the peptide, the N-terminal amino group, and the rapidly off-exchanging N-terminal amide from the number of peptide amide residues in a given peptide (*29, 30*). Figure 2 shows peptide aa sequence number, while Figures 3-7 and Supplemental Material show the locations of exchange-assessable amides in peptide probes. In general, the number of exchange-assessable amides is two less than the number of amino acid residues in a peptide. Three independent experiments were performed for each condition and the results presented in figures for individual peptides are the mean and standard error calculated from these triplicate experiments.

RESULTS

Recombinant Lp-PLA$_2$ expression, activity measurement and interfacial binding

All C-terminal 6xHis tagged, N-terminal 6xHis tagged and N-terminal enterokinase cleavable GST tagged Lp-PLA$_2$s (residues 46-441) were expressed in *E. coli* strain BL-21. We found that the N-terminal 6xHis tagged protein showed weak binding affinity toward nickel affinity beads, thus it was not suitable for the purification. The C-terminal 6x-His tagged protein was purified, but showed a 80% reduction of activity toward the substrate PAF compared to the GST cleaved Lp-PLA$_2$. Disturbance of the C-terminal region by the His tag seemed to affect the enzyme's activity. Hence, the GST cleaved Lp-PLA$_2$ was utilized in our experiments. The purified Lp-PLA$_2$ had a specific activity of 200 *μmol/min/ mg*, a value similar to those reported elsewhere (*6, 31, 32*). The interfacial binding of Lp-PLA$_2$ was monitored by protein tryptophan fluorescence (Figure 1). Fluorescence labeled lipid N-dansyl-DHPE was used as a probe and mixed with 60 μM DMPC. The binding reaction was initiated by adding increasing amounts of recombinant Lp-PLA$_2$ protein. As shown in Figure 1, the energy transfer reached a maximum when 2 μM protein was loaded. The lipid/protein ratio is about 30, a value similar to the reported one (*27*).

Lp-PLA$_2$ digestion coverage map

The protein digestion procedure was optimized to produce a peptide map that yielded the best coverage by assessing varying denaturant concentrations, flow rates and pepsin incubation times. The optimized condition at 0.5 M guanidine hydrochloride, protease column flow rate of 0.1 ml/min, with 40 s pepsin contact time, allowed us to identify 92 high quality peptides. This optimized condition gave a total of 94% coverage of the recombinant Lp-PLA$_2$. Among these 92 peptides, 33 peptides (shown in Figure 2 as solid lines) with the best signal to noise ratio and least overlapping regions were selected for representation of the H/D exchange data in figures 3, 4 and Supplemental Material. However, all 92 peptides were analyzed in each experiment and the exchange data for all peptides was found to be in agreement with the 33 selected peptides.

Amide H/D Exchange Dynamics of Lp-PLA$_2$ Alone and Bound to DMPC vesicles

Lp-PLA$_2$ alone or previously admixed with DMPC vesicles was supplemented with D$_2$O buffer to 75% D$_2$O and aliquots exchange-quenched in formic acid, 0.5 M guanidine hydrochloride at intervals from 10 s to 10,000 s. Quenched samples were frozen at -80°C, later thawed at 4°C, and subjected to pepsin proteolysis with subsequent LCMS performed under exchange-quench conditions. The only significant difference in deuteration between Lp-PLA$_2$ alone or previously admixed with DMPC vesicles was in peptides that included the Lp-PLA$_2$ region containing amides 113-120 (see Figure 3, 4, and Supplemental Material Figure S1). Figure 3 is a ribbon-diagram representation of the percent of maximal deuterium incorporation that occurred in probe peptides during the several deuteration durations employed with free Lp-PLA$_2$ (upper ribbon) and liposome-bound Lp-PLA$_2$ (lower ribbon). In this figure, only the peptide containing exchange-assessable amides 113-120 of Lp-PLA$_2$ accumulated deuterium significantly more slowly in the presence of DMPC vesicles than in their absence. Figure 4 demonstrates that the three probe peptides that cover this Lp-PLA$_2$ region (those with exchange-assessable amides 107-121, 113-121, and 113-123) all incorporated two deuterons less at early time points in the presence of DMPC vesicles, and that this slowing in exchange persisted through the longest on-exchange durations assessed. Peptide probes immediately flanking this region (those with amides 98-110, 121-139) showed identical deuterium incorporation with and without DMPC vesicles, as did all other peptides assessed throughout Lp-PLA$_2$ (see Supplemental Material, Figure S1).

The region of Lp-PLA$_2$ containing amides 113-120, consists of 8 amides, two of which are significantly slowed in exchange rate by the presence of DMPC vesicles. Among the eight residues in this region, Trp-115 and Leu-116 are the most hydrophobic and would be expected to make a large contribution in an interaction with a DMPC vesicle surface. To examine the roles of these residues in the binding of Lp-PLA$_2$ with phospholipid membranes, both Trp-115 and Leu-116 were replaced by alanine residues to create a W115A/L116A double mutant. After confirming that the double mutant retained most of its enzymatic activity (Fig.5A), DXMS experiments were performed as they had been done on the wild-type protein to test whether this double mutation would affect the interaction between the protein and lipid membranes. We found that the region of the double mutant containing amides 113-120 had no difference in exchange rate with or without DMPC lipid vesicles (Fig. 5B), in contrast to the two amide slowing in the wild-type protein in the presence of DMPC vesicles. We have also carried out a lipid vesicle binding experiment using the W115AL116A mutant. As shown in Figure 1, the mutant showed significantly decreased fluorescence compared with the wild-type protein.

Region 362-369 contains mostly hydrophobic residues, which form an α-helix located on the protein surface, and this region has been shown to influence protein/HDL binding *(33)*. Thus it has been proposed that two α-helixes (including residues 114-126 and 362-369), mediate Lp-PLA$_2$-lipoprotein association and comprise the interfacial binding surface (*15*). In our DXMS experiments, we did not detect any changes in deuteration behavior in the region that covers residues 362-369 of Lp-PLA$_2$ in the presence of DMPC lipid vesicles under conditions in which the other α-helix shows that vesicles are bound (Figure 6).

DISCUSSION

Functions of Lp-PLA$_2$

GVIIA PLA$_2$ has received a great deal of attention in recent years because it circulates primarily with LDL and HDL lipoproteins and is increasingly referred to as Lp-PLA$_2$. Lp-PLA$_2$ has broad substrate specificity for acyl chains up to 9 methylene groups at the *sn*-2 position of phospholipids (*9*). The involvement of oxidized LDL in the inflammatory process within vulnerable atherosclerotic lesions indicates the importance of Lp-PLA$_2$ in atherosclerosis *(34)*. In vulnerable plaque regions, Lp-PLA$_2$ acts on the oxidized phospholipids to generate the pro-inflammatory lysoPC and oxidized fatty acids. Because Lp-PLA$_2$ is implicated in atherosclerosis, inhibiting its activity is thought to be beneficial for the treatment of cardiovascular diseases. One reversible inhibitor, GSK SB-480848 has been reported to potentially reduce complex coronary atherosclerotic plaque development in the porcine model and now is in phase III human studies *(35)*. To better understand the activation mechanism of Lp-PLA$_2$, we have used DXMS to yield both structural information in solution and information about the dynamics of the enzyme-phospholipid surface interactions. The on-exchange experiments with the recombinant Lp-PLA$_2$ showed a good correlation between the crystal structure and the deuteration level of Lp-PLA$_2$. Our DXMS results suggest that the C-terminal residues 430-441 were not able to be crystallized due to the high flexibility in this region. This region showed more than 90% exchange in 10s in our DXMS experiments (Figure 3). Actually the C-terminus is very important for maintaining enzyme activity. Removal of 21 amino acids from the C-terminal residues caused a slight loss of activity, but a 30 residue deletion reduced catalysis to below the limit of detection (*14*). We also found that addition to the C-terminal of a 6xHis tag reduces more than 80% of the enzyme activity. The additional hydrophilic histidines on the C-terminal may affect protein-substrate and/or protein-lipid interactions. Amino acids 114-116 were found disordered in the apo-protein crystal structure and these residues were also detected by DXMS. They showed complete exchange after 50 min, which reflects the flexibility of these residues on the protein surface. A large group of regions around the active site, including

residues 256-282, 285-295 and 348-357, form a hydrophobic pocket and the residues detected in this region barely exchanged even after 10,000 s. We have shown a slow deuteration rate in the active site, indicating that the active site located in this hydrophobic pocket is not solvent accessible and exhibits very low flexibility.

Interaction with lipid vesicles

The interfacial activation mechanism of PLA_2 enzymes has been an area of interest for many years. Although $Lp-PLA_2$ was suggested to act by a non-interfacial mechanism toward the substrate PAF in early days (*27*), recent research has shown that $Lp-PLA_2$ may also take substrates from the lipid phase since it is exclusively bound to lipoproteins in human plasma (*36*). Experiments carried out in the presence of DMPC SUVs showed decreases of H/D exchange at the region 113-120. This region is mostly composed of hydrophobic amino acids except residues His-114 and Asn-119. This is consistent with previous findings that the interaction between $Lp-PLA_2$ and lipid vesicles was not predominantly electrostatic because addition of 0.5 M NaCl did not cause the dissociation of $Lp-PLA_2$ from lipid vesicles (*27*). His-114, the apparently polar and charged residue was predicted as a neutral form penetrating into the nonpolar phase of lipid membranes (*37*). A significant decrease of H/D exchange (2 deuterons decrease) was found in this region.

Trp-115 and Leu-116 are the most hydrophobic residues in this region and have been suggested to be critical for $Lp-PLA_2$ association with LDL particles (*37*). This implies that Trp-115 and Leu-116 may mediate penetration of the enzyme into the lipid membrane surface. To test this hypothesis, we replaced both tryptophan and leucine with alanine. The W115A/L116A double mutant showed only somewhat decreased enzymatic activity compared with the wild-type protein. However, DXMS experiments with the W115A/L116A $Lp-PLA_2$ showed that the H/D exchange level of region 113-120 was not decreased by the presence of DMPC lipid vesicles in contrast to the control enzyme. Also the mutant shows dramatically reduced affinity to DMPC lipid vesicles when monitoring the resonance energy transfer from $Lp-PLA_2$ tryptophans to the probe *N*-dansyl-DHPE present as a minor component in DMPC lipid vesicles. All together this confirms that Trp-115/Leu-116 plays a key role in $Lp-PLA_2$/phospholipid association, suggesting that substrate does not have to be transferred to the enzyme directly from vesicles.

Residues 362-369 together with residues 114-126, the two α-helixs on the protein surface, were suggested to comprise the interfacial binding surface (*15*). However, our DXMS experiments did not detect any deuteration level changes upon binding with DMPC lipid vesicles in the region that covers residues 362-369.

From these results, we propose that $Lp-PLA_2$ and lipid binding is only mediated by the region composed of residues 113-120. Trp-115 and Leu-116 are key residues for $Lp-PLA_2$/lipid interaction and they may penetrate into lipid membranes during association. A hypothetical model of the membrane association of $Lp-PLA_2$ is shown in Figure 7. In our model, the active site opens to the solvent and faces the interfacial surface that accesses substrates from the lipoprotein particles. The active site would theoretically allow substrates to enter from the aqueous phase as well as substrates partitioning into the lipoproteins. The current identified binding interface contains the same region as the region that has been proposed to contribute to $Lp-PLA_2$/LDL interaction (residues 114-126) (*37*).

Comparison with other PLA_2s

$Lp-PLA_2$ is an α/β hydrolase reminiscent of a neutral lipase, distinct from the other known phospholipase A_2s which do not conform to this type of α/β hydrolase fold (*3*). $Lp-PLA_2$ distinguishes itself from all other enzymes of the PLA_2 superfamily not only in structure but

also in substrate specificity. Lp-PLA$_2$ and its homologues (GVIIB PAF-AHII and GVIII PLA$_2$) prefer the short acyl group at the *sn*-2 position of phospholipids while all the other enzymes are more active toward a long acyl group at the *sn*-2 position of phospholipids. This raises the question as to whether the Lp-PLA$_2$ binds to lipid membrane surfaces differently than other PLA$_2$s.

The H/D exchange experiments described herein provide insight into the differences in the interfacial binding properties compared with the other classic PLA$_2$s in our previous studies (*20-22, 24*). Unlike Lp-PLA$_2$, the secreted PLA$_2$s are smaller in size and relatively planar structures. There are no specific regions implicated at the interfacial binding surfaces but only residues along the surface contribute to the binding. GIA PLA$_2$, a Ca^{2+}-dependent 13 KDa secreted form, utilizes the aromatic residues Tyr-3, Trp-61, Tyr-63 and Phe-64 to penetrate into the membrane bilayer when binding to a lipid surface (*21*). Other sPLA2s, which show more activity toward anionic phospholipids, were thought to bind the membrane interface mainly by electrostatic interactions (*42*). For instance, the recent crystal structure of GIB sPLA$_2$ in a premicellar complexes has shown that the enzyme uses the hydrophilic residues Arg-6 and Lys-10 to bind at the anionic interface (*43*).

GIVA cytosolic Ca^{2+}-dependent PLA$_2$ (cPLA$_2$), which contains a C2 (Ca^{2+} binding) domain and a catalytic domain, needed both the C2 and catalytic domains to bind to the lipid membrane. A lid region on the catalytic domain opens upon binding to the lipid and then allows the substrate access to the active site. The hydrophobic regions on the C2 domain residues 35-39 and 96-98 as well as Trp-464 on the catalytic domain penetrate into the membrane surface (*20*). The electrostatic contacts between Lys-273, Arg-274, and Arg-467 on the catalytic domain and the polar head groups on the lipid membrane would also help protein-lipid binding (*20*). The most striking difference between the binding surface of Lp-PLA$_2$ and that of GIVA cPLA$_2$ is that the additional C2 domain of GIVA cPLA$_2$ is crucial for enzyme binding to the lipid membranes.

The interaction pattern between Lp-PLA$_2$ and lipid membranes is similar to that of GVIA Ca^{2+}-independent PLA$_2$ (iPLA$_2$). Although GVIA iPLA$_2$ has seven ankyrin repeats in addition to the catalytic domain, only the residues on the catalytic domain are involved in membrane localization (*24*). Both GVIA iPLA$_2$ and Lp-PLA$_2$ lack a cap or lid region compared with GIVA cPLA$_2$ and their active sites are more accessible to the solvent. Owing to their "open" active site architecture, GVIA iPLA$_2$ and GVIIA Lp-PLA$_2$ appear to be less discriminatory for the *sn*-2 acyl chains of phospholipid substrates.

In conclusion, we have employed peptide amide hydrogen-deuterium exchange mass spectrometry (DXMS) to characterize, at the molecular level, the association of Lp-PLA$_2$ with lipid membranes, and found that specific residues (aa 113-120) in one of the enzyme's surface-disposed hydrophobic α-helices likely mediates liposome binding. Mutagenesis study has shown that Trp-115 and Leu-116 are important for Lp-PLA$_2$ binding to lipid membranes.

Supplementary Material

Refer to Web version on PubMed Central for supplementary material.

Acknowledgments

Abbreviations

Lp-PLA$_2$	Lipoprotein-associated phospholipase A$_2$
LDL	low-density lipoproteins
HDL	high-density lipoproteins
DMPC	1,2-dimyristoyl-*sn*-glycero-3-phosphocholine
DXMS	hydrogen deuterium exchange mass spectrometry
PAF	platelet activating factor
PC	phosphocholine
CHAPS	3-[(3-cholamidopropyl) dimethylammonio]-1-propanesulfonate
IPTG	isopropyl-β-thiogalactopyranoside

REFERENCES

1. McIntyre TM, Prescott SM, Stafforini DM. The emerging roles of PAF acetylhydrolase. J Lipid Res 50 Suppl. 2009:S255–259.

2. Stafforini DM, Prescott SM, McIntyre TM. Human plasma platelet-activating factor acetylhydrolase. Purification and properties. J Biol Chem. 1987; 262:4223–4230. [PubMed: 3558407]

3. Schaloske RH, Dennis EA. The phospholipase A2 superfamily and its group numbering system. Biochim Biophys Acta. 2006; 1761:1246–1259. [PubMed: 16973413]

4. Stremler KE, Stafforini DM, Prescott SM, McIntyre TM. Human plasma platelet-activating factor acetylhydrolase. Oxidatively fragmented phospholipids as substrates. J Biol Chem. 1991; 266:11095–11103. [PubMed: 2040620]

5. Min JH, Wilder C, Aoki J, Arai H, Inoue K, Paul L, Gelb MH. Platelet-activating factor acetylhydrolases: broad substrate specificity and lipoprotein binding does not modulate the catalytic properties of the plasma enzyme. Biochemistry. 2001; 40:4539–4549. [PubMed: 11294621]

6. Stafforini DM, Sheller JR, Blackwell TS, Sapirstein A, Yull FE, McIntyre TM, Bonventre JV, Prescott SM, Roberts LJ 2nd. Release of free F2-isoprostanes from esterified phospholipids is catalyzed by intracellular and plasma platelet-activating factor acetylhydrolases. J Biol Chem. 2006; 281:4616–4623. [PubMed: 16371369]

7. Shimizu T. Lipid mediators in health and disease: enzymes and receptors as therapeutic targets for the regulation of immunity and inflammation. Annu Rev Pharmacol Toxicol. 2009; 49:123–150. [PubMed: 18834304]

8. Prescott SM, Zimmerman GA, Stafforini DM, McIntyre TM. Platelet-activating factor and related lipid mediators. Annu Rev Biochem. 2000; 69:419–445. [PubMed: 10966465]

9. Stafforini DM. Biology of platelet-activating factor acetylhydrolase (PAF-AH, lipoprotein associated phospholipase A2). Cardiovasc Drugs Ther. 2009; 23:73–83. [PubMed: 18949548]

10. Stafforini DM. Functional Consequences of Mutations and Polymorphisms in the Coding Region of the PAF Acetylhydrolase (PAF-AH) Gene. Pharmaceuticals. 2009; 2:94–117.

11. Casas JP, Ninio E, Panayiotou A, Palmen J, Cooper JA, Ricketts SL, Sofat R, Nicolaides AN, Corsetti JP, Fowkes FG, Tzoulaki I, Kumari M, Brunner EJ, Kivimaki M, Marmot MG, Hoffmann MM, Winkler K, Marz W, Ye S, Stirnadel HA, Khaw KT, Humphries SE, Sandhu MS, Hingorani AD, Talmud PJ. PLA2G7 Genotype, Lipoprotein-Associated Phospholipase A2 Activity, and Coronary Heart Disease Risk in 10 494 Cases and 15 624 Controls of European Ancestry. Circulation. 2010

12. Wilensky RL, Macphee CH. Lipoprotein-associated phospholipase A(2) and atherosclerosis. Curr Opin Lipidol. 2009; 20:415–420. [PubMed: 19667981]

13. Burke JE, Dennis EA. Phospholipase A2 structure/function, mechanism, and signaling. J Lipid Res 50 Suppl. 2009:S237–242.

14. Tjoelker LW, Eberhardt C, Unger J, Trong HL, Zimmerman GA, McIntyre TM, Stafforini DM, Prescott SM, Gray PW. Plasma platelet-activating factor acetylhydrolase is a secreted phospholipase A2 with a catalytic triad. J Biol Chem. 1995; 270:25481–25487. [PubMed: 7592717]

15. Samanta U, Bahnson BJ. Crystal structure of human plasma platelet-activating factor acetylhydrolase: structural implication to lipoprotein binding and catalysis. J Biol Chem. 2008; 283:31617–31624. [PubMed: 18784071]

16. Gelb MH, Min JH, Jain MK. Do membrane-bound enzymes access their substrates from the membrane or aqueous phase: interfacial versus non-interfacial enzymes. Biochim Biophys Acta. 2000; 1488:20–27. [PubMed: 11080673]

17. Woods VL Jr. Hamuro Y. High resolution, high-throughput amide deuterium exchange-mass spectrometry (DXMS) determination of protein binding site structure and dynamics: utility in pharmaceutical design. J Cell Biochem Suppl Suppl. 2001; 37:89–98.

18. Konermann L, Tong X, Pan Y. Protein structure and dynamics studied by mass spectrometry: H/D exchange, hydroxyl radical labeling, and related approaches. J Mass Spectrom. 2008; 43:1021–1036. [PubMed: 18523973]

19. Engen JR. Analysis of protein conformation and dynamics by hydrogen/deuterium exchange MS. Anal Chem. 2009; 81:7870–7875. [PubMed: 19788312]

20. Burke JE, Hsu YH, Deems RA, Li S, Woods VL Jr. Dennis EA. A phospholipid substrate molecule residing in the membrane surface mediates opening of the lid region in group IVA cytosolic phospholipase A2. J Biol Chem. 2008; 283:31227–31236. [PubMed: 18753135]

21. Burke JE, Karbarz MJ, Deems RA, Li S, Woods VL Jr. Dennis EA. Interaction of group IA phospholipase A2 with metal ions and phospholipid vesicles probed with deuterium exchange mass spectrometry. Biochemistry. 2008; 47:6451–6459. [PubMed: 18500818]

22. Hsu YH, Burke JE, Stephens DL, Deems RA, Li S, Asmus KM, Woods VL Jr. Dennis EA. Calcium binding rigidifies the C2 domain and the intradomain interaction of GIVA phospholipase A2 as revealed by hydrogen/deuterium exchange mass spectrometry. J Biol Chem. 2008; 283:9820–9827. [PubMed: 18211893]

23. Burke JE, Babakhani A, Gorfe AA, Kokotos G, Li S, Woods VL Jr. McCammon JA, Dennis EA. Location of inhibitors bound to group IVA phospholipase A2 determined by molecular dynamics and deuterium exchange mass spectrometry. J Am Chem Soc. 2009; 131:8083–8091. [PubMed: 19459633]

24. Hsu YH, Burke JE, Li S, Woods VL Jr. Dennis EA. Localizing the membrane binding region of Group VIA Ca2+-independent phospholipase A2 using peptide amide hydrogen/deuterium exchange mass spectrometry. J Biol Chem. 2009; 284:23652–23661. [PubMed: 19556238]

25. Stafforini DM, McIntyre TM, Prescott SM. Platelet-activating factor acetylhydrolase from human plasma. Methods Enzymol. 1990; 187:344–357. [PubMed: 2172738]

26. Adam J, Bateman L. Control stimuli in investigations of the acute-angled and obtuse-angled Muller-Lyer illusions. Perception. 1980; 9:467–474. [PubMed: 7422463]

27. Min JH, Jain MK, Wilder C, Paul L, Apitz-Castro R, Aspleaf DC, Gelb MH. Membrane-bound plasma platelet activating factor acetylhydrolase acts on substrate in the aqueous phase. Biochemistry. 1999; 38:12935–12942. [PubMed: 10504265]

28. Zhang Z, Smith DL. Determination of amide hydrogen exchange by mass spectrometry: a new tool for protein structure elucidation. Protein Sci. 1993; 2:522–531. [PubMed: 8390883]

29. Bai Y, Milne JS, Mayne L, Englander SW. Primary structure effects on peptide group hydrogen exchange. Proteins. 1993; 17:75–86. [PubMed: 8234246]

30. Hamuro Y, Anand GS, Kim JS, Juliano C, Stranz DD, Taylor SS, Woods VL Jr. Mapping intersubunit interactions of the regulatory subunit (RIalpha) in the type I holoenzyme of protein kinase A by amide hydrogen/deuterium exchange mass spectrometry (DXMS). J Mol Biol. 2004; 340:1185–1196. [PubMed: 15236976]

31. Tew DG, Southan C, Rice SQ, Lawrence MP, Li H, Boyd HF, Moores K, Gloger IS, Macphee CH. Purification, properties, sequencing, and cloning of a lipoprotein-associated, serine-dependent phospholipase involved in the oxidative modification of low-density lipoproteins. Arterioscler Thromb Vasc Biol. 1996; 16:591–599. [PubMed: 8624782]

32. Kruse S, Mao XQ, Heinzmann A, Blattmann S, Roberts MH, Braun S, Gao PS, Forster J, Kuehr J, Hopkin JM, Shirakawa T, Deichmann KA. The Ile198Thr and Ala379Val variants of plasmatic PAF-acetylhydrolase impair catalytical activities and are associated with atopy and asthma. Am J Hum Genet. 2000; 66:1522–1530. [PubMed: 10733466]

33. Gardner AA, Reichert EC, Topham MK, Stafforini DM. Identification of a domain that mediates association of platelet-activating factor acetylhydrolase with high density lipoprotein. J Biol Chem. 2008; 283:17099–17106. [PubMed: 18434304]

34. Macphee CH, Nelson J, Zalewski A. Role of lipoprotein-associated phospholipase A2 in atherosclerosis and its potential as a therapeutic target. Curr Opin Pharmacol. 2006; 6:154–161. [PubMed: 16495153]

35. Wilensky RL, Shi Y, Mohler ER 3rd, Hamamdzic D, Burgert ME, Li J, Postle A, Fenning RS, Bollinger JG, Hoffman BE, Pelchovitz DJ, Yang J, Mirabile RC, Webb CL, Zhang L, Zhang P, Gelb MH, Walker MC, Zalewski A, Macphee CH. Inhibition of lipoprotein-associated phospholipase A2 reduces complex coronary atherosclerotic plaque development. Nat Med. 2008; 14:1059–1066. [PubMed: 18806801]

36. Pande AH, Tillu VA. Membrane lipid composition differentially modulates the function of human plasma platelet activating factor-acetylhydrolase. Biochim Biophys Acta. 2010

37. Stafforini DM, Tjoelker LW, McCormick SP, Vaitkus D, McIntyre TM, Gray PW, Young SG, Prescott SM. Molecular basis of the interaction between plasma platelet-activating factor acetylhydrolase and low density lipoprotein. J Biol Chem. 1999; 274:7018–7024. [PubMed: 10066756]

38. Tellis CC, Tselepis AD. The role of lipoprotein-associated phospholipase A2 in atherosclerosis may depend on its lipoprotein carrier in plasma. Biochim Biophys Acta. 2009; 1791:327–338. [PubMed: 19272461]

39. Stafforini DM, Carter ME, Zimmerman GA, McIntyre TM, Prescott SM. Lipoproteins alter the catalytic behavior of the platelet-activating factor acetylhydrolase in human plasma. Proc Natl Acad Sci U S A. 1989; 86:2393–2397. [PubMed: 2928339]

40. Stafforini DM, McIntyre TM, Carter ME, Prescott SM. Human plasma platelet-activating factor acetylhydrolase. Association with lipoprotein particles and role in the degradation of platelet-activating factor. J Biol Chem. 1987; 262:4215–4222. [PubMed: 3549727]

41. Stafforini DM, Prescott SM, Zimmerman GA, McIntyre TM. Mammalian platelet-activating factor acetylhydrolases. Biochim Biophys Acta. 1996; 1301:161–173. [PubMed: 8664325]

42. Winget JM, Pan YH, Bahnson BJ. The interfacial binding surface of phospholipase A2s. Biochim Biophys Acta. 2006; 1761:1260–1269. [PubMed: 16962825]

43. Pan YH, Bahnson BJ. Structure of a premicellar complex of alkyl sulfates with the interfacial binding surfaces of four subunits of phospholipase A2. Biochim Biophys Acta. 2010; 1804:1443–1448. [PubMed: 20302975]
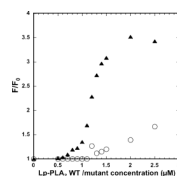
Figure 1. Lipid vesicle binding
60 μM DMPC containing 3 mol% N-danyl-DHPE were mixed with the indicated amount of
Lp-PLA$_2$ wild-type (▲) or W115AL116A mutant (○) and F/F$_0$ were determined.
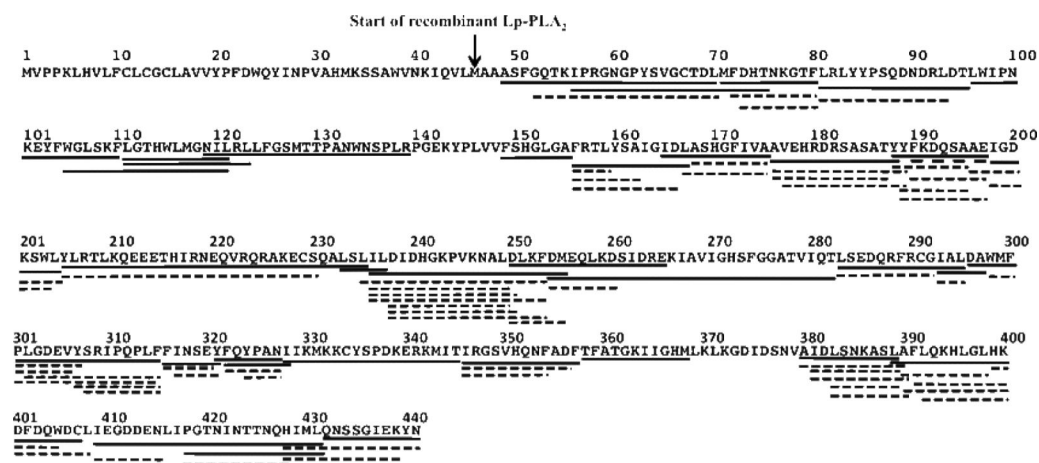
Figure 2. Peptide probe coverage map of Lp-PLA₂
Probe peptides produced by optimal pepsin digestion LC-MS are shown underneath the primary sequence of Lp-PLA₂. Deuteration results for the 33 peptides represented by solid lines are shown in Figures 3-6 and Supplemental Material Figure S1.
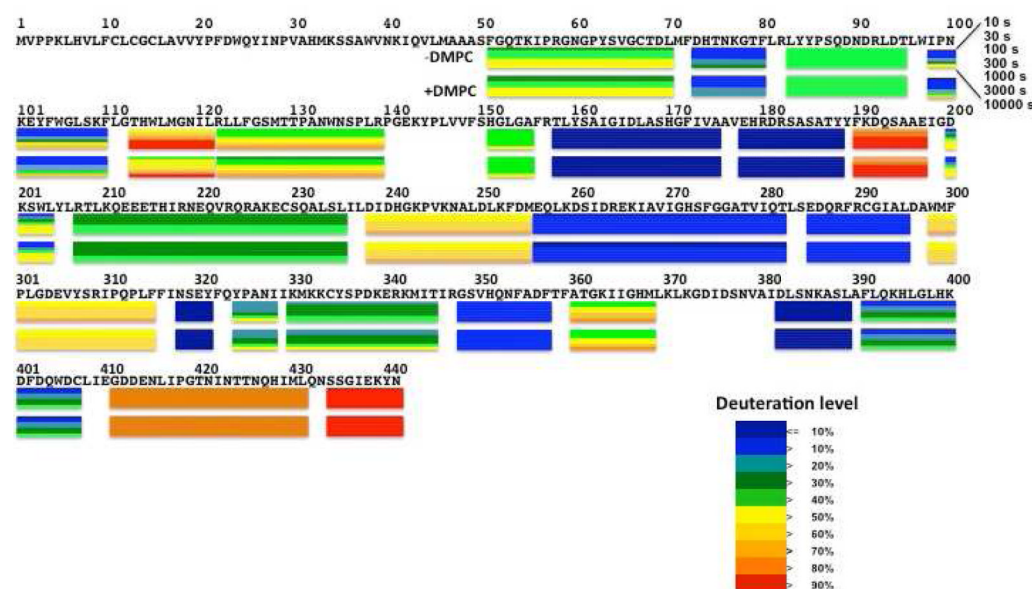
Figure 3. Amide hydrogen/deuterium exchange analysis of Lp-PLA2 free and associated with DMPC vesicles

The percent of maximal deuterium incorporation into Lp-PLA2 peptidic regions alone (upper ribbon) or with DMPC vesicle incubation (lower ribbon) is shown. In each ribbon, the percent deuteration at each of the labeling durations is shown from 10 to 10,000 s (top to bottom). Differential coloring indicates the percentage of maximal labeling in a given time period.
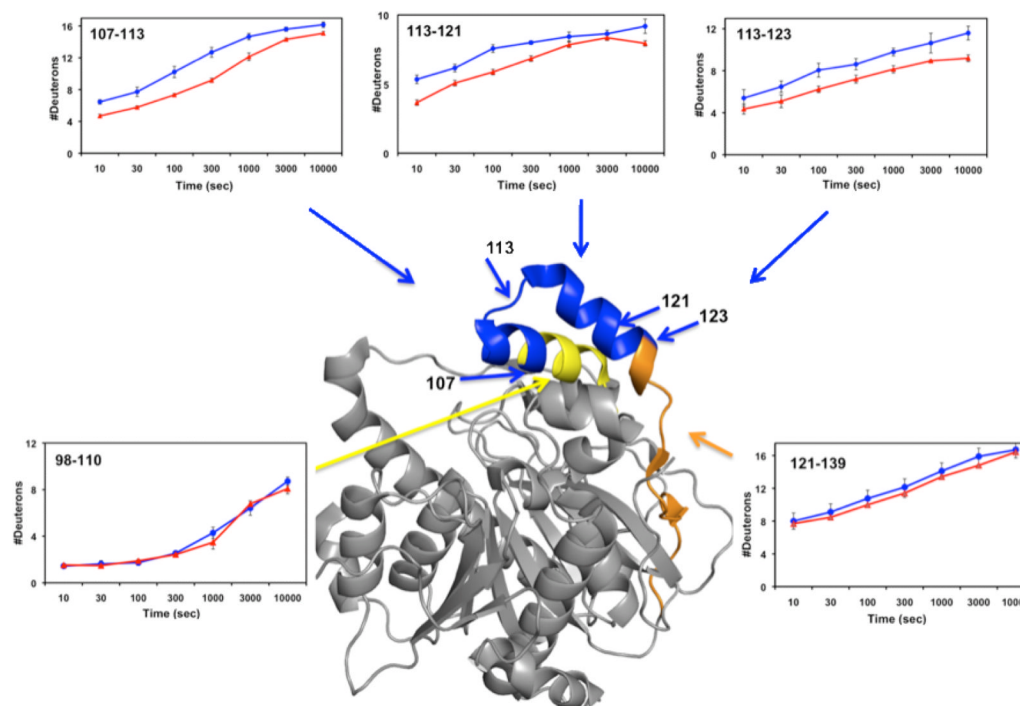
Figure 4. Deuterium exchange of Lp-PLA$_2$ upon association with DMPC lipid vesicles
The number of incorporated deuterons at each of seven time points from 10s to 10,000s in Lp-PLA$_2$ alone (●) and Lp-PLA$_2$ in the presence of DMPC (▲) are plotted for Lp-PLA$_2$ peptides containing amides 98-110, 107-121, 113-121, 113-123 and 121-139. The scale of the y axis is the number of incorporated deuterons. S.E. (bar) was determined in three individual experiments.
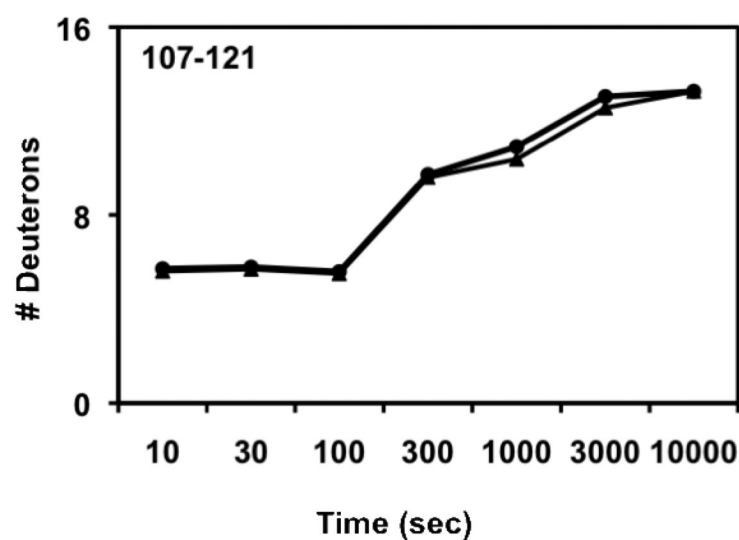
A.
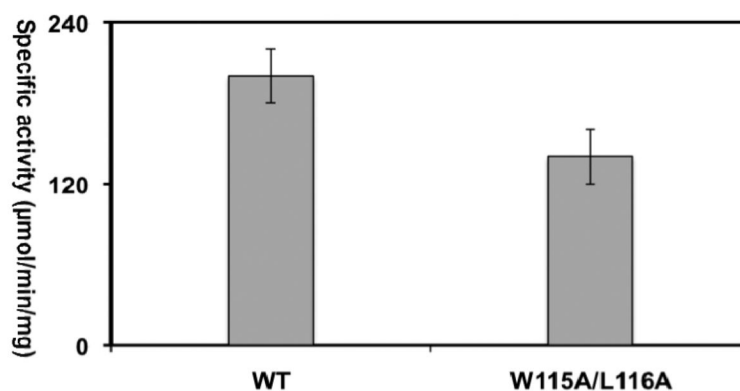
B.

Figure 5. Effect of tryptophan 115 and leucine 116 double mutation on enzyme activity and exchange behavior
Panel A repersents the enzymatic activity of wild type (WT) and mutant Lp-PLA$_2$ (mean +- S.E. of triplcate determinations). Panel B shows the deuterium incorporation into the amide 107-121 region of double mutant Lp-PLA$_2$ in isolated Lp-PLA$_2$ (●) and Lp-PLA$_2$ in the presence of DMPC vesicles (▲) . Legend is otherwise as indicated in Figure 4.
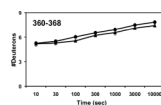
Figure 6. Deuterium exchange of Lp-PLA$_2$ upon binding with DMPC lipid vesicles in the region containing exchange-assessable amides 360-368
The numbers of incorporated deuterons at seven time points in Lp-PLA$_2$ (●) and Lp-PLA$_2$ with DMPC (▲) are plotted for region 360-368. The scale of the y axis is the number of incorporated deuterons. S.E. (bar) was determined by three individual experiments.
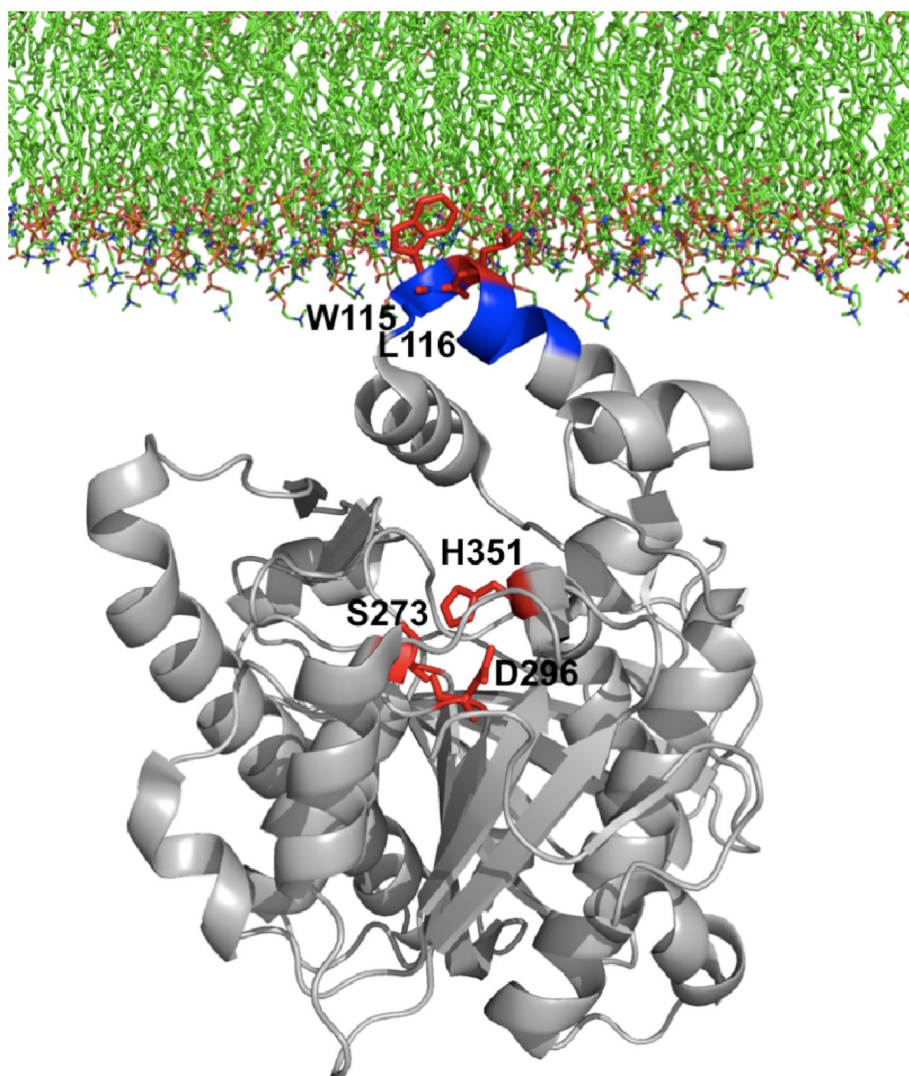
Figure 7. Hypothetical model of Lp-PLA$_2$ association with the DMPC lipid membrane surface
The Lp-PLA$_2$ region implicated in the present study (amides113-120), is shown in blue and the as the proposed key residues for Lp-PLA$_2$/liposome association, W115 and L116 are shown in red, as are the catalytic triad residues, S273, D296 and H351.